Vibrational Spectroscopy, Photochemistry, and Photophysics of Molecular Clusters†

FRANCIS G. CELII‡ and KENNETH C. JANDA*§

Arthur Amos Noyes Laboratory for Chemical Physics, California Institute of Technology, Pasadena, California 91125

Received October 30, 1985 (Revised Manuscript Received January 16, 1986)

Contents

I. Introduction 507
II. Triatomic Molecules 508
A. Ar–H_2 508
B. Ar–HCl 509
III. Linear-Molecule Dimers 509
A. HF Dimer 509
B. HCl Dimer 510
C. HCN Dimer 510
D. NO Dimer 510
E. N_2O, CO_2, and C_2H_2 Dimers 510
IV. Noble Gas–Polyatomic Dimers 510
A. Noble Gas–OCS 511
B. Noble Gas–C_2H_4 511
V. Polyatomic–Polyatomic Dimers 511
A. NH_3 Dimers 511
B. C_2H_4 Dimers 512
C. C_3H_4 Dimer 513
D. CH_3OH Dimer 513
E. SiF_4 Dimer 513
F. CF_3Br and CF_3I Dimers 513
G. H_2O Dimer 516
H. C_6H_6 Dimer 516
VI. Large Clusters 516
A. Rare Gas Clusters 516
B. Homogeneous Molecular Clusters 519
C. Isotope Separation with Clusters 519
VII. Summary 519

I. Introduction

The observation and interpretation of the infrared spectra of van der Waals molecules and clusters is a rapidly expanding field. Van der Waals molecules provide a unique medium for state-to-state studies of vibrational energy transfer rates. By preparing a vibrationally excited molecule via supersonic expansion and laser excitation, the initial state quantum numbers can be well-defined. Transfer of energy into the van der Waals modes results in dissociation of the molecule. In principle, the dynamics for each possible final state can be followed using a probe laser to determine the energy in the fragments. In practice, such pump–probe experiments in the infrared are made difficult by the paucity of tunable infrared lasers and the relative insensitivity of infrared detectors. To date, most information on energy transfer in these weakly bound species is a result of recording the infrared absorption or dissociation spectrum of a dimer and inferring dynamics from line shapes and spectral simulation. The homogeneous line width yields information on the relaxation rate through the uncertainty principle: fast rates of relaxation imply uncertainty in the energy and result in a broadened transition.

Experiments in the visible portion of the spectrum which probe energy transfer within van der Waals molecules are substantially easier and are reviewed elsewhere in this volume. Studies of van der Waals complexes in the infrared region are worth the extra effort because they provide examples of phenomena which occur unambiguously on a single electronic surface. Frequency shifts and dynamics can be clearly attributed to the vibrational part of the wave function. This statement cannot be made with assurance for the electronic excited states of even the simplest molecules.

This article focuses on the literature from July 1983, until June 1985, a narrow range of time which serves to update our previous review.[1] Our perception of vibrational dynamics has changed dramatically over these past 2 years. When ref 1 was submitted, most infrared spectra of clusters consisted of broad bands that were interpreted as evidence for fast intramolecular energy redistribution. To some extent, this was due to the prevalence of dissociation spectroscopy employing CO_2 lasers, the discrete nature of which favors the detection of broad features, with the exception of accidental coincidences between a laser line (FWHM ~ 150 MHz) and a narrow spectral transition. Recently, several groups have succeeded in using continuously tunable lasers to obtain high resolution, rotationally resolved spectra of dimers which indicate the preparation of metastable vibrational levels of the weakly bound molecules. The observation of these narrow spectral features puts a burden of proof on those who claim to have observed lifetime broadened spectral lines to show that no experimental errors (e.g., inhomogeneity in the line shape due to the superposition of profiles from several complexes) are involved. The majority of this review will concentrate on the issue of obtaining true dynamical information from line width measurements.

The use of van der Waals molecules as prototypical systems for the study of intramolecular energy redistribution received an initial boost from the seminal study of the He–I_2 molecule by Levy, Wharton, and Smalley.[2] Levy et al.[2] inferred the rates for energy transfer from the I_2 vibration to the He–I_2 bond which results in predissociation of the van der Waals complex. The energy transfer rate as a function of the I_2 vibrational state could be modeled quite accurately with a

† Contribution No. 7353 from the California Institute of Technology.
‡ Current address: Institut für Physikalisch Chemie, Universität Basel, CH-4056 Basel, Switzerland.
§ Current address: Department of Chemistry, University of Pittsburgh, Pittsburgh, PA 15260.

0009-2665/86/0786-0507$06.50/0

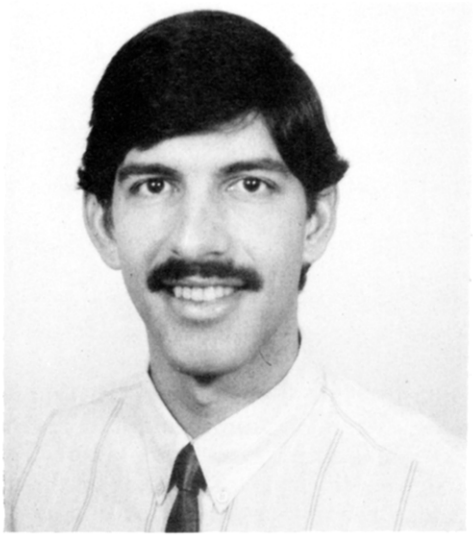

Francis G. Celii was born in Downingtown, PA. He received his B.A. in chemistry and physics from LaSalle College (Philadelphia) and his Ph.D. in chemistry from the California Institute of Technology, with Kenneth C. Janda. He is presently a postdoctoral fellow at the University of Basel with Prof. J. P. Maier. His research interests include photochemistry of surface adsorbates, vibrational spectroscopy of van der Waals molecules, and electronic spectroscopy of ions.

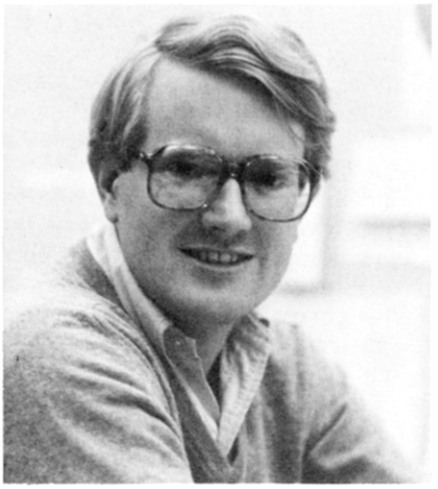

Kenneth Janda was born in Denver, Colorado. He obtained an A.B. degree from Hope College, Holland, Michigan. His Ph.D. studies were performed under William Klemperer at Harvard University. After an NSF postdoctoral fellowship with Lennard Wharton at the University of Chicago he studied van der Waals molecule structure and dynamics at the California Institute of Technology. During this time he received fellowships from the A. P. Sloan Foundation, the Camille and Henry Dreyfus Foundation, and the Fulbright Foundation. Ken is now an Associate Professor of Chemistry at the University of Pittsburgh.

Golden Rule type model based on a simple V–T mechanism.[3] The results are characterized as being due to "energy gap"[3] or "momentum gap"[4] constraints on the energy-transfer pathway. The larger the energy difference between the I_2 vibrational quantum, which supplies the energy for the dissociation, and the van der Waals bond modes, which accept the energy, the harder (exponentially!) it is to couple the two modes. This explains the fact that for He–I_2, excitation of $v = 26$ (in the B state) results in vibrational predissociation within 38 ps while the lifetime of He–I_2 excited to the $v = 12$ (B state) level is 220 ps. Even more dramatic is the case of Ne–Cl_2, for which the lifetime of the excited dimer in the $v = 12$ level of the B state (where $\omega_{12-11} = 130$ cm^{-1}) is 50 ps, while excited in the $v = 1$ state of the ground (X state) surface ($\omega_{1-0} = 550$ cm^{-1}) the complex lives for over 10^{-5} s[5]. An increase of a factor of three in the vibrational frequency in this case slows the energy-transfer rate by over five orders of magnitude.

The energy gap rule is, of course, best utilized when comparing similar systems, so extrapolations to other molecules must be made with care. Also, for systems more complicated than triatomics like He–I_2, excitation of other degrees of freedom (rotational as well as other vibrational modes) will be important as a means of reducing the energy gap. Besides the energy gap, the coupling strength of the two vibrational modes will dramatically affect the energy-transfer rates.[4,6] One purpose of the work which we review here is to gather a body of data to assess the importance of these variouis factors. Unfortunately, high-level calculations are only feasible for the triatomic examples. This severely hinders (at present) the understanding of vibrational relaxation in polyatomic van der Waals molecules.

During the past 3 years, several reports of remarkably detailed observations on polyatomic dimer predissociation have appeared. Pine and co-workers have measured rotationally resolved absorption spectra for Ar–HCl,[7] $(HF)_2$,[8] and $(HCl)_2$[9] which indicate that predissociation from HX stretching motions in these molecules is generally rather slow, with $\tau > 10^{-9}$ s. Hayman et al.[10] have obtained resolved spectra of rare gas–OCS dimers that show similarly long-lived vibrationally excited states. Fraser et al.[11] have determined infrared–microwave double resonance spectra for several NH_3 dimers which indicate that dissociation rates for these molecules are strongly dependent on the NH_3 bonding partner. These experiments, as well as the others reviewed here, show that detailed data are now available on intramolecular vibrational relaxation rates for rather complex molecules.

The last section of the review will focus on recent results and interpretations of the infrared bands of large van der Waals clusters. An overall goal of the work on large van der Waals molecules is to assess the comparability of molecules in clusters to those in condensed phases. An exciting development in this vein is the ability of the Waterloo group to obtain the IR spectrum of a chromophore (SF_6) located on the outside edge of a large Ar cluster.[12] Work in our own lab[13] shows that even a simple property such as the fundamental frequency of a molecule absorbed in a rare gas cluster does not change smoothly from its gas phase to its matrix value as the size of the cluster increases. The Lausanne group[14] has demonstrated the usefulness of large clusters as isotope separation media. Rare gas clusters may provide models of surfaces to increase our understanding of properties of adsorbed molecules, while large homogeneous clusters can be studied as models of condensed media.

II Triatomic Molecules

A. Ar–H_2

The predissociation of Ar–H_2 is probably the most completely studied van der Waals molecule system.[6] Results on Ar–H_2 and the other rare gas–hydrogen complexes have been extensively reviewed.[1,6,15] The

potential energy surface has been well characterized, both spectroscopically[16] and by inelastic scattering.[17] Energy transfer from the high-frequency H_2 stretch (4150 cm^{-1}) to the modes of the van der Waals bond is almost certainly too slow to be observed by conventional techniques. The dynamics which are observed are due instead to energy transfer from the Ar–H_2 internal rotation mode to the weak bond. Simulation of this prototypical system has shown that the dissociation lifetimes are very sensitive not only to the overall "energy gap" or "momentum gap", but also to the details of the potential energy surface.[6,15] The calculations also demonstrate that a wide variety of open and closed exit channels must be included before the calculated resonance width can be considered to be converged.[6,18]

B. Ar–HCl

Besides the rare gas–hydrogen complexes, the rare gas–hydrogen halides, especially Ar–HCl, are the only other group for which the potential energy surface has been well-determined. Direct spectroscopy on the van der Waals vibrational motions has also recently been performed.[19] Pine and Howard[7] have recorded the Ar–HCl absorption spectrum in the HCl stretching region. Although no lifetime broadening is observed in the low rotational levels, broadening due to rotational predissociation is seen in transitions between high rotational levels. Unfortunately, the HCl stretch is, like that of H_2, so high in frequency that it transfers energy very slowly to the low-frequency modes in Ar–HCl. Thus for the two types of molecules for which theory is most practical, vibrational predissociation has not been observed. The calculations of Hutson,[20] however, predict that while vibrational predissociation of Ar–HCl occurs too slowly to be observed in line broadening, it may be detected by using time-of-flight measurements.

III. Linear-Molecule Dimers

A. HF Dimer

The dimer of HF is the tetraatomic system about which the most information is currently available. The HF dimer contains an almost linear hydrogen bond with the external (nonbonded) proton bent well off the heavy-atom axis.[21,22] Potential energy surfaces[23-25] for the molecule have been obtained using precise rotational constants, centrifugal distortion, and tunneling splitting measurements for $(HF)_2$, $(DF)_2$, HF–DF, and DF–HF. Excitation of either the HF or DF stretch can lead to dissociation of the complex. The infrared spectrum has been recorded in the region of the HF (DF) stretching frequencies using both absorption[8] and beam attenuation[26,27] techniques. In the absorption spectra, Pine et al.[8] observe no line broadening of the nonbonded ν_1 stretch of HF(DF) in $(HF)_2$, DF–HF, or $(DF)_2$. Modeling of the absorption spectra lead to a determination that $\tau > 10$ ns, while the photodissociation work of DeLeon and Muenter[26] indicates a longer lifetime limit of $\tau > 30$ ns. Broadening of the bonded HF(DF)ν_2 stretch absorption line is observed in $(HF)_2$ but not in DF–HF or $(DF)_2$. Molecular-beam laser-dissociation spectra[27] attributed to $(HF)_2$ contain two bands in agreement with the results of Pine[8] plus an additional sharp resonance at 3720 cm^{-1}. Andrews[28] has assigned this third transition as due to an open $(HF)_3$ configuration on the basis of concentration and diffusion dependences of the absorption intensity of this band in the spectra of Ar and Ne matrices containing HF.

The line-broadening results indicate that, while excitation of the HF ν_2 stretch in $(HF)_2$ results in a larger "energy gap" for dissociation than DF excitation in HF–DF, HF–HF* has a shorter vibrational lifetime than HF–DF*. A simple V–T dissociation model is not able to reconcile these results. Such a model predicts that the lifetime of $(DF)_2$* should be 10^3 times shorter than $(HF)_2$*, yet line broadening indicates $(HF)_2$* ($\nu_2 = 1$) is the shorter lived of the two excited dimers. Considering a V–T,R mechanism, Ewing[29] has predicted that the higher moment of inertia of DF relative to HF would result in similar lifetimes for HF–HF* and DF–DF*. To see how this can come about, consider the following simple model calculation. For $(HF)_2$ and $(DF)_2$ the excitation frequencies of the internal hydrogen bond stretches (ν_2) are approximately 3870 and 2830 cm^{-1}, respectively.[8] The bond energy is about 1040 cm^{-1},[23] so the energy which must be dispersed in the product exit channel is 2830 and 1790 cm^{-1}, respectively. The energy gap constraints in a V–T mechanism would hinder HF–HF* dissociation compared to DF–DF*. Ewing[4] argues that angular momentum gap constraints should operate in such a way that the dissociation rate will decrease dramatically as the product rotational quantum numbers increase. If the product energy is divided equally between the two constituent rotational degrees of freedom, HF–HF* would dissociate to give HF ($J = 8$) whereas DF–DF* dissociation would yield DF ($J = 9$). The larger moment of inertia of DF compensates for the smaller energy gap in dissociation of $(DF)_2$, so DF–DF* is predicted to dissociate more slowly than HF–HF* by taking the product rotational excitation into consideration.

An interesting question regarding the decay times deduced from these spectra is whether intermediate states play a role in line broadening. For instance, instead of the single-step dissociation mechanism (1)

$$\text{HF*–DF} \rightarrow \text{HF } (v = 0, J) + \text{DF } (v = 0, J') \quad (1)$$

intramolecular energy transfer may be involved

$$\text{HF*–DF} \rightarrow \text{HF–DF*} \ (v_{\text{stretch}} = 1, v_{\text{bend}} = n_b) \quad (2a)$$

$$\text{HF–DF*} \ (1, n_b) \rightarrow \text{HF } (v = 0, J) + \text{DF } (v = 0, J') \quad (2b)$$

In the second mechanism, the initial HF excitation first relaxes to a combination of the DF stretch and the bending and/or stretching modes of the hydrogen bond. Such a mechanism has been postulated[30] to be responsible for dissociation of larger dimers, but unfortunately the spectra of mixed HF–DF dimers in the HF ν_1 or ν_2 excitation region, for which this channel would be open, have not been reported.

Another explanation for the observed line broadening results is that the high- and low-frequency vibrations of the DF dimer are more weakly coupled than the corresponding modes in the HF dimer, due to the smaller amplitude of motion of the DF stretch compared with the HF stretch.[8b] More sophisticated calculations may provide a conclusive explanation for the unexpected ordering of dissociation lifetimes in the HF and DF dimers. Halberstadt et al.[29b] have shown that

adding the rotational degree of freedom to a close coupling calculation of the HF dimer dissociation does yield a dissociation rate consistent with the experimental line width. In this calculation, the HF dimer was treated as a quasitriatomic molecule, with the free hydrogen atom not included in the calculation. As predicted by Ewing's arguments, the results show that the dissociation would yield highly rotationally excited products, with the $J = 9$ and $J = 10$ channels being predominant.

The IR absorption spectrum of the HCN–HF molecule in the region of the HF stretch has been studied by Kyrö et al.[31] They observe rotationally structured bands for both the hydrogen-bonded HF stretch, ν_1, and the sequence band, $\nu_6 + \nu_1 - \nu_6$, where ν_6 is the hydrogen bond bending mode. Simulation of the broadened line shapes results in an estimate of 200 ps for the vibrational lifetime of the excited dimers.

B. HCl Dimer

Ohashi and Pine[9] have recorded the infrared spectrum of HCl dimer in the region near the HCl stretching frequencies, 2850–2950 cm^{-1}. As with HF dimer, the spectrum shows a well-resolvd rotational structure which will be useful for creating a precise potential energy surface. With the possibility of obtaining additional information from substitution of the Cl isotopes, the HCl dimer may ultimately yield more detailed knowledge regarding vibrational predissociation dynamics than the HF dimer.

There is no broadening in the reported HCl dimer spectrum[9] which can be attributed to vibrational predissociation. This implies that the vibrationally excited dimer has a longer lifetime than that of HF–HF*, in which the internal HF stretch is excited. The ordering of lifetimes is contrary to a simple V–T energy gap law. Since the internal HCl stretching frequency of HCl dimer is ~2855 cm^{-1} and the dimer bond energy is only 430 cm^{-1},[23] the energy to be dissipated is about 2400 cm^{-1}, 85% of the excess energy in $(HF)_2$* dissociation, which implies a shorter lifetime for $(HCl)_2$* compared to $(HF)_2$*. The HCl rotational constant is roughly one-half that of HF, however, so the angular momentum gap (see the discussion of HF dimer) is considerably greater for the HCl dimer than the HF dimer: HCl ($J = 11$) would be produced from $(HCl)_2$* whereas HF($J = 8$) removes the excess product energy from $(HF)_2$*, assuming energy equilibration among the dimeric constituents. This calculation predits $(HCl)_2$* will have a longer lifetime than $(HF)_2$*, as observed. As was also seen in the case of HF and DF dimers, the experimental ordering of lifetimes can also be explained on the basis of the coupling between high- (HF vs. DF stretches) and low-frequency modes. The coupling is expected to be weaker in $(HCl)_2$ since the van der Waals bond strength is less than half that of $(HF)_2$.

C. HCN Dimer

An experimental difficulty in the infrared region is the limited number of laser sources which can be used to excite molecular vibrations. Dyke and co-workers[32] have attempted to surmount this problem by using the CARS technique which they utilized in the study of HCN dimer and trimer. They have successfully recorded bands in the CN stretch region (2105 cm^{-1}) which are several wavenumbers wide. The monomer rotational temperature under their beam conditions was measured to be 160 K, and thus it is likely the dimer band is highly inhomogeneous. Although the experiment does not reveal new predissociation lifetime data, it does raise hopes of obtaining spectra for a variety of modes which are presently inaccessible. The CARS technique has also been previously employed to detect mixed $Ar_n(C_2H_4)_m$ clusters.[33]

D. NO Dimer

Three groups have studied the infrared absorption and photodissociation spectrum of NO dimer.[34-36] The structure of $(NO)_2$ is known to be trapazoidal with the monomers bonded between the N atoms.[37] The asymmetric combination of the NO stretching motions (1785 cm^{-1}) should strongly couple to the low-frequency modes of the dimer since the rotational constants are observed to increase by about 1% upon vibrational excitation, and this change has been attributed to the out-of-phase dipole–dipole interaction.[36] In spite of the predicted strong coupling, the excited state lifetime of $(NO)_2$* is estimated to be greater than 100 ps, from both modeling of the rotational band shape in absorption,[35,36] and the paucity of overlap between the spectral lines and the discrete emission lines of the CO laser which is used to effect dissociation.[36]

E. N_2O, CO_2, and C_2H_2 Dimers

Miller et al. have reported sharp rotational structure in the spectra of N_2O dimer,[38b] CO_2 dimer,[39] and C_2H_2 dimer[40,41] excited in the 3000–4000 cm^{-1} region. In each case, individual transitions with line widths near the instrumental limit of 3 MHz were observed which imply lifetimes of greater than 80 ns. In addition, several bands in the spectrum of $(C_2H_2)_2$ between 3250 and 3300 cm^{-1} exhibit line widths of up to 90 MHz ($\tau = 1.6 \times 10^{-9}$ s). In the case of irradiation of CO_2 dimer in the $\upsilon_1 + \upsilon_3$ region, substantial excitation of the ν_2 bending mode occurs due to Fermi resonance. Interestingly, Miller et al.[39] note that $(OCS)_2$*, a dimer which would be expected to be quite similar in structure and bonding to CO_2 dimer, directly excited into the overtone of the ν_2 mode,[42] dissociates 10^4 times faster than $(CO_2)_2$* excited in the $\nu_1 + \nu_3$ region.

The lifetime limit for N_2O dimer excited in the $\upsilon_1 + \upsilon_3$ band is much longer than the 1–100 ps range previously estimated[39] from spectra obtained by using molecular beams containing predominantly large N_2O clusters. This situation is by no means an isolated instance and highlights a continual problem in this field, that of van der Waals molecule detection: at present, no detector is specifically sensitive to a particular cluster size (see, however, the recent work of Klemperer[11] and Buck[43] and co-workers). Only when rotational structure can be assigned is the cluster size assignment truly verified.

IV. Noble Gas–Polyatomic Dimers

The final class of molecules for which rotational structure has been assigned in the infrared region is that of noble gas atoms bound to polyatomics, specifically OCS[10] and C_2H_4.[44,45] Certainly this group is not a fundamental limit since rotational structure is observed

in the vibronic spectrum of much larger molecules.[46] In the infrared, Klemperer and co-workers[11] have observed narrow transition line widths for several dimers of NH_3, and sharp structure has been reported for propyne dimers by Miller et al.[41] Rather, the lack of resolved spectra and concomitant structural determination for most large molecules is another indication of the relative difficulty of obtaining conclusive dimer spectra in the infrared region.

A. Noble Gas–OCS

It has been previously reported that the Ar–OCS transition near the free OCS bending mode overtone ($2\nu_2$, 1046 cm^{-1}) is broadened to 1.0 cm^{-1} (τ = 5 ps) by intramolecular relaxation.[42,47] Transitions in the ν_3 stretch region (2063 cm^{-1}), on the other hand, exhibit no lifetime broadening at 10^{-3} cm^{-1} resolution.[10] The two results are consistent with energy gap arguments for either a V–T or a V–R,T dissociation mechanism. Ar–OCS* (ν_3 = 1) might be expected to quickly relax via a V–V′,R,T mechanism, leaving the OCS fragment vibrationally excited, but apparently this is not the case. It is not surprising that the ν_2 bending mode should more strongly couple to the weak van der Waals bond of the "T"-shaped Ar–OCS molecule than the ν_3 stretch.

A quasiclassical simulation[48] of the $2\nu_2$ excitation of Ar–OCS was unable to reproduce the rapid vibrational predissociation which has been inferred from dissociation line shapes.[42,47] We are again presented with the quandary of whether to believe that the experimental measurement represents a homogeneously broadened transition or rather that the profile is significantly inhomogeneous. Indeed, the observed intensity of the Ar–OCS transition is only 15% of that expected from the free OCS $2\nu_2$ intensity which suggests that narrow features are hidden between the CO_2 laser used to effect the dissociation. It would certainly be of great value to confirm the measurement of this broad band with a tunable laser.

No evidence for broadening due to vibrational predissociation is detected in the IR absorption spectrum of OCS–rare gas dimers in the OCS ν_3 stretch region, recorded by Hayman et al.[10] For polyatomic molecules it is often impossible to calculate a true potential energy surface, so it is thus important when simple models can explain observed trends. Reuss and co-workers[49] have developed one such theory to explain the splitting of the ν_3 (940 cm^{-1}) transition of the SF_6 dimer. The model includes the dipole moment of the infrared transition in the dipole-induced dipole perturbation treatment of the attractive part of the van der Waals potential. Hayman et al.[10] likewise find agreement between the results of the Reuss model and the observed shift of the X–OCS ν_3 vibrational frequency as a function of the polarizability of the rare gas bonding partner X, although simple electrostatic arguments[50] should likewise succeed in explaining the observed trend in this case.

B. Noble Gas–C_2H_4

Of the experiments reviewed above, only the spectra of the HF dimer show well-resolved and assigned rotational structure with line broadening which can be unambiguously attributed to vibrational predissociation. The success of a hindered rotor model to fit the observed Ne–C_2H_4 dissociation spectrum (Figure 1)[44] suggests that Ne–C_2H_4 may eventually, with higher resolution spectra, be similarly analyzed. The transition excited in the spectrum shown in Figure 1 corresponds to the ν_7 out-of-plane bending mode of free C_2H_4. Although the dimer spectrum has been probed with only a line-tunable CO_2 laser, the narrow structure throughout the profile is obvious. The absolute photodissociation intensity indicates that the transition has a line width on the order of 0.1 cm^{-1}. Likewise, in the ν_9 and ν_{11} C–H stretch region (3000 cm^{-1}) of Ar–C_2H_4, Liu et al.[45] have identified rotational structure. No evidence for line broadening is observed which, similar to the ν_7 excitation results, suggests relaxation dynamics with $\tau > 10^{-11}$ s.

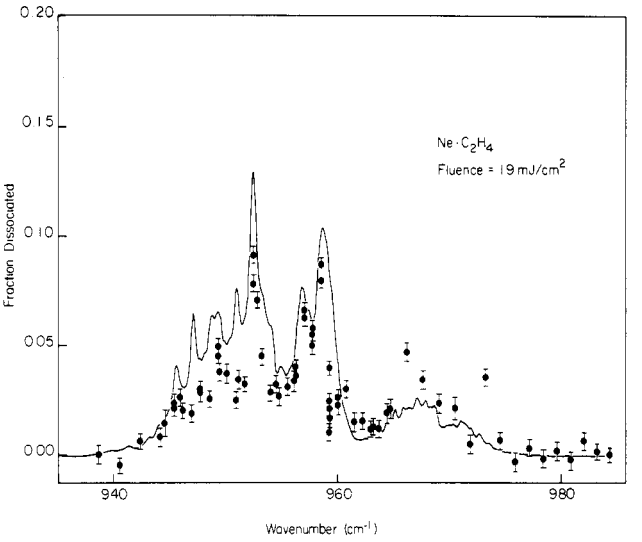

Figure 1. Observed predissociation spectrum of Ne–C_2H_4 in the ν_7 region of free C_2H_4. A spectral simulation using a hindered rotor model is included.[44]

Hutson, Clary, and Beswick[51] performed a dynamical simulation of Ne–C_2H_4 and Ar–C_2H_4 excited in the ν_7 mode and conclude that both molecules relax on the picosecond timescale via a V–V′,R,T mechanism, where V′ indicates excitation of the ν_{10} torsional mode of free C_2H_4 at 810 cm^{-1}. However, both the C–H stretch[45] and C–H bend[44] mode spectra indicate that the rare gas atom is located *in the plane* of the C_2H_4 rather than *out of plane* as calculated with an atom–atom potential used in the dynamical simulation.[51] Presumably, use of the in-plane geometry in the calculations would lead to a slower dissociation rate. Indeed, if the calculations are within an order of magnitude of the true rate, both Ne–C_2H_4 and Ar–C_2H_4 are excellent choices for high-resolution study since the dynamics predicted are fast enough to result in line broadening, but not so fast as to obscure rotational structure.

V. Polyatomic–Polyatomic Dimers

A. NH_3 Dimers

Fraser et al.[11] have reported novel studies of NH_3 dimers using a double resonance technique employing a microwave oscillator and a CO_2 laser in a molecular beam electric resonance (MBER) spectrometer. As with the previous double resonance dissociation of $(HF)_2$,[26] the infrared laser excites transitions from single rotational levels of a specific dimer—there is no doubt in

TABLE I. Infrared Origins, Line Widths and Excited-State Lifetimes of NH_3 Dimers[11]

dimer	ν_0, cm^{-1} [a]	Γ, cm^{-1}	τ, s
NH_3–C_2H_2	984.4 (9)	0.005	10^{-9}
NH_3–CO_2	987.1 (2)	0.45 (20)	10^{-11}
NH_3–OCS	981.5 (1.5)	0.30	10^{-11}
NH_3–N_2O	980.0 (2)	0.30	10^{-11}
NH_3–Ar	(939)[b]	0.01	10^{-10}
NH_3–NH_3	987.9 (8)	5.2, 3.5	10^{-12} [c]

[a] The inversion-free ν_2 transition frequency of free gas-phase NH_3 occurs at 950.3 cm^{-1}. The unquenched inversion doublet occurs at 931.58 and 968.08 cm^{-1}.[11] [b] This transition is not directly comparable to the others; see text. [c] This may be an underestimate; see text.

this case that the molecule which is probed is the dimer of interest. The detailed microwave spectra which were also obtained provide accurate molecular structures which can be used for simulation of the infrared bands. With no possibility of rotational congestion, any observed line width of the transitions must be due to homogeneous broadening. The energy transfer rate out of the ν_2 umbrella mode of NH_3 is found to vary dramatically as a function of the weak-binding partner. Table I summarizes the observed transition frequencies, line widths and lifetimes for this study. Notice, for instance, that vibrationally excited NH_3*–C_2H_2 has a lifetime of 10^{-9} s while that of NH_3*–CO_2 is on the order of 10^{-11} s.

For NH_3–C_2H_2 a single infrared transition is observed at 984.38 cm^{-1} in double resonance with the $J = 4$, $K = 1$ level of the ground vibrational state. No other rotational level could be excited with the discrete emission lines of the CO_2 laser. The line width of the transition was estimated[11] to be $\Gamma = 0.005$ cm^{-1} from consideration of the probability of observing only one IR resonance, given simulation of the spectral profile and an estimate of the rotational temperature. The line width thus corresponds to an excited vibrational state lifetime of $\tau = 10^{-9}$ s.

In contrast, the double-resonance results for the dimers of NH_3 with CO_2, OCS, and N_2O are quite different from those of NH_3–C_2H_2. Each NH_3–CO_2 rotational level probed with the microwave radiation can be excited with one or more CO_2 laser transitions. The ν_2 line width for both NH_3–OCS and NH_3–N_2O appear to be quite similar to that of NH_3–CO_2 inferring relaxation dynamics in the 10^{-11} s range for these three dimers, two orders of magnitude shorter than the lifetime of NH_3–C_2H_2*. N_2O and OCS are isoelectronic and are expected to bond to NH_3 in a geometry similar to CO_2. The bonding is different in NH_3–OCS and NH_3–CO_2, as indicated by the disparity of the NH_3 ν_2 transition frequencies (981 and 987 cm^{-1} respectively), but this does not seem to affect the dynamics appreciably. Lastly, the $2\nu_2$ bending mode of OCS in the NH_3–OCS dimer can also be excited, and the line width of the transition was found to be 0.1–1.0 cm^{-1}, in good agreement with line widths of other OCS dimers measured by Gentry and co-workers,[42,47] who did not employ the dimer-specific double-resonance technique.

As with NH_3–C_2H_2, only one isolated double resonance was found in the Ar–NH_3 dimer. The transition which overlaps the CO_2 laser emission spectrum occurs at 938.69 cm^{-1}, over 40 cm^{-1} removed from the ν_2 transition frequency of the other dimers studied (Table I), and close to that of an unquenched inversion transition of free NH_3. The infrared transition frequency corroborates other evidence that Ar–NH_3 is a nearly free rotor.[11] The line width is estimated to be even narrower than that of the NH_3–C_2H_2 transition.

The infrared spectrum of the NH_3 dimer shows an interesting doublet structure related to the two distinct monomers in the complex. While the components exhibit slightly different line widths, both are broader than those of the other NH_3 dimers. Although the transitions are observed in double resonance, Fraser et al.[11] still consider the possible inhomogeneous contributions due to internal motions of the dimer. Also, there is experimental[52] and theoretical[53] evidence to suggest that the bond strength of $(NH_3)_2$ is greater than that provided by a single CO_2 laser photon (2.8 kcal/mol). The reported results would then be consistent with dissociation of an excited-state dimer (hot band). Given the observed signal intensities, the authors[11] consider this possibility unlikely and thus determine that the bond strengths of the studied NH_3 dimers are less than 2.8 kcal/mol.

B. C_2H_4 Dimers

The dimer of C_2H_4 was the first complex to show a broad, homogeneous infrared absorption band,[54,55] and has subsequently become one of the most extensively studied species. This system has been the subject of several previous reviews.[1,30,56] The ν_7 symmetric out-of-plane bending mode of $(C_2H_4)_2$ apparently relaxes on a subpicosecond timescale, yielding an intrinsic line width of about 10 cm^{-1}. Recent work by Buck[43b] utilizing crossed molecular beam scattering for cluster selection corroborates assignment of this band to the dimer. A broad ($\sim$5 cm^{-1}) band in the ν_9 region (3105 cm^{-1}) of free C_2H_4, probed with a continuous narrowband (150 MHz) F-center laser, exhibits no sharp rotational structure, likewise suggesting picosecond relaxation dynamics in the dimer.[41]

Gentry[30,52] has argued that the extremely fast vibrational relaxation of the various C_2H_4 dimers, together with the small amount of product translational energy, indicates that the observed line broadening is due to intramolecular energy redistribution and not vibrational predissociation. Using a pump–probe technique, Mitchell et al.[57] were able to establish an upper limit of 10^{-8} s on the dissociation timescale of ν_7-excited $(C_2H_4)_2$, but this leaves a broad range of four orders of magnitude between the real-time measurement limit[57] and the line width derived lifetime.[55] Certainly there is a dimer size for which intramolecular relaxation will be much faster than predissociation (e.g., see section V.D.), but it still remains to establish what that size is.

We hold the view[56] that the various relaxation rates in the series of C_2H_4 dimers can be qualitatively explained using the angular momentum propensity arguments of Ewing.[4] Spectra which illustrate the range of line widths we have observed are shown in Figure 2. The observed line width of the C_2H_4 ν_7 transition decreases successively by an order of magnitude as the C_2H_4 binding partner in the dimer is changed from C_2H_4 to HCl to Ne. We also note that the line width variation in the C_2H_4 system is similar to that observed for NH_3 dimers:[11] the narrowest line widths, and hence longest vibrational lifetimes, are observed in the rare gas complexes, while the broadest line widths are ex-

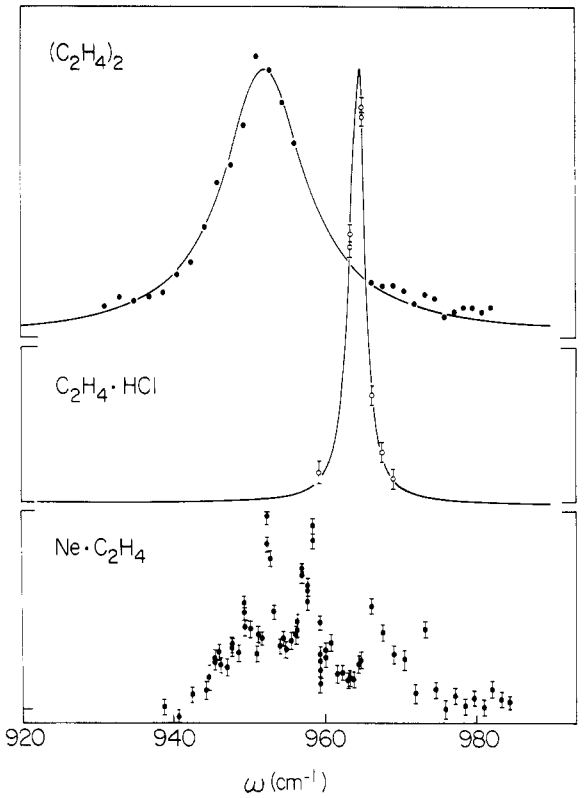

Figure 2. Observed vibrational predissociation spectra of (a) $(C_2H_4)_2$; (b) C_2H_4–HCl; (c) C_2H_4–Ne. The line widths of the transition narrow by two orders of magnitude in this sequence of C_2H_4 binding partners.[50]

hibited by the homogeneous dimers, $(C_2H_4)_2$ and $(NH_3)_2$.

King and Stephenson[58] have used UV laser excited fluorescence to probe the NO rotational and translational energy distributions that result from dissociation of C_2H_4–NO following excitation at 953 cm^{-1}. Their results are consistent with Boltzmann distributions of population in the NO modes. The NO rotational states can be characterized by a temperature of $T_r = 75 \pm 15$ K which indicates that the average energy released into rotation is 50 cm^{-1}. The translational energy distribution, obtained from the Doppler profile of the NO transitions, is fit by $T_t \sim 100$ K, indicating an average translational energy of 100 cm^{-1}. That only 150 cm^{-1} of the 550 cm^{-1} total product energy appears in the NO fragment indicates that dissociation occurs rapidly (i.e., by a direct mechanism) and precludes statistical randomization of the internal energy. On the other hand, the fact that the population of the NO fragment modes can be characterized by Boltzmann distributions suggests that the dissociation mechanism is not dominated by specific product channels as would be predicted by an "energy gap" analysis.[4] This experiment is certainly an important initial determination of the fragment internal excitation following infrared excitation of a van der Waals molecule, but more data of this type are needed to understand the mechanism of dissociation in the C_2H_4 dimers.

C. C_3H_4 Dimer

Fischer et al.[41] have observed rotational structure in the ν_1 (acetylenic C–H stretch) region of propyne dimer, $(C_3H_4)_2$. Using a tunable F-center laser at 5 MHz resolution, line widths of 0.01 cm^{-1} ($\tau > 0.4$ ns) were recorded although not assigned. While the propyne molecule is similar in vibrational complexity to ethylene, the excited propyne dimer lives 100–1000 times longer than the excited ethylene dimer.[55]

TABLE II. CF_3I and CF_3Br Transition Frequencies[a]

mode	dissoc.[b]	gas-phase[c]	CF_3X/Ar[d]	CF_3X/Ne[e]
		CF_3I		
$\nu_2+\nu_3$	1027.3	1028.0	1027.5	----
ν_1	1074.6	1075.0	1065.0	----
$2\nu_5$	1080.5	1080.8	1069.2	----
dimer($\nu_1/2\nu_5$)	1076/1081[f]	----	1074/1077	----
	1069/—[g]	----	----	----
trimer(ν_1)	----	----	1083.5	----
		CF_3Br		
ν_1	1085.2	1084.6	1076.0	1081.4
$2\nu_5$	>1092.5[h]	1095.6	1092.5	1094.1
dimer(ν_1)	1086.2[f]	----	1099.0	----
	1078.6[g]	----	1095.0	----
$\nu_2+\nu_3$	----	1112.0	1116.8	1119.1

[a] All values in cm^{-1}. [b] Vibrational predissociation spectra, Ar–CF_3X dimers (this work). [c] From Fuss.[64] [d] From Jacox.[63] [e] From Bürger et al.[65] [f] "Free" CF_3I moiety. [g] "Bound" CF_3I moiety. [h] From Geraedts et al.[60]

D. CH_3OH Dimer

Hoffbauer et al.[59] have measured a very broad (13.8 cm^{-1}) band for excitation of CH_3OH dimer in the C–O stretch region (1050 cm^{-1}). With only 0.2% of the excitation energy appearing as translation of the fragments, they interpret the line width to be indicative of fast intramolecular vibrational relaxation, exclusive of the vibrational predissociation rate, as they concluded for C_2H_4-containing dimers. Since $(CH_3OH)_2$ is relatively strongly bound, it is certainly a good candidate for preparation of a long-lived metastable complex in which the excitation energy is randomized throughout all modes of the dimer prior to dissociation.

E. SiF_4 Dimer

The predissociation spectrum of SiF_4 dimer[60] in the Si–F stretch region exhibits two absorption features (only one is completely resolved) which correspond to splitting of the threefold degenerate ν_3 mode, analogous to the previously reported case of SF_6 dimer.[49,61] The resolved component in the CO_2 laser dissociation spectrum of $(SiF_4)_2$ is broader than those measured for $(SF_6)_2$ ($\Gamma = 4.7$ and 1.5 cm^{-1}, respectively). The lower limit on the lifetime of the excited SiF_4 dimer is thus shorter than that for SF_6 dimer ($\tau = 1.1$ and 3.5 ps, respectively), but nothing more conclusive can be ventured as to the relaxation time.

F. CF_3Br and CF_3I Dimers

We have determined the predissociation spectra of van der Waals complexes containing either CF_3Br or CF_3I.[62] Given the available low-frequency modes in the monomer, one might expect rapid vibrational relaxation in the dimers. Besides the intense ν_1 vibration which can be excited in both monomers, the $\nu_2 + \nu_3$ combination band and the $2\nu_5$ overtone (in Fermi resonance with the ν_1 mode) can also be probed in CF_3I dimers within the tuning range of the CO_2 laser. A summary of the results obtained for these clusters is given in Table II. Although the spectra are collected near the sensitivity limit of our spectrometer, it is not clear that

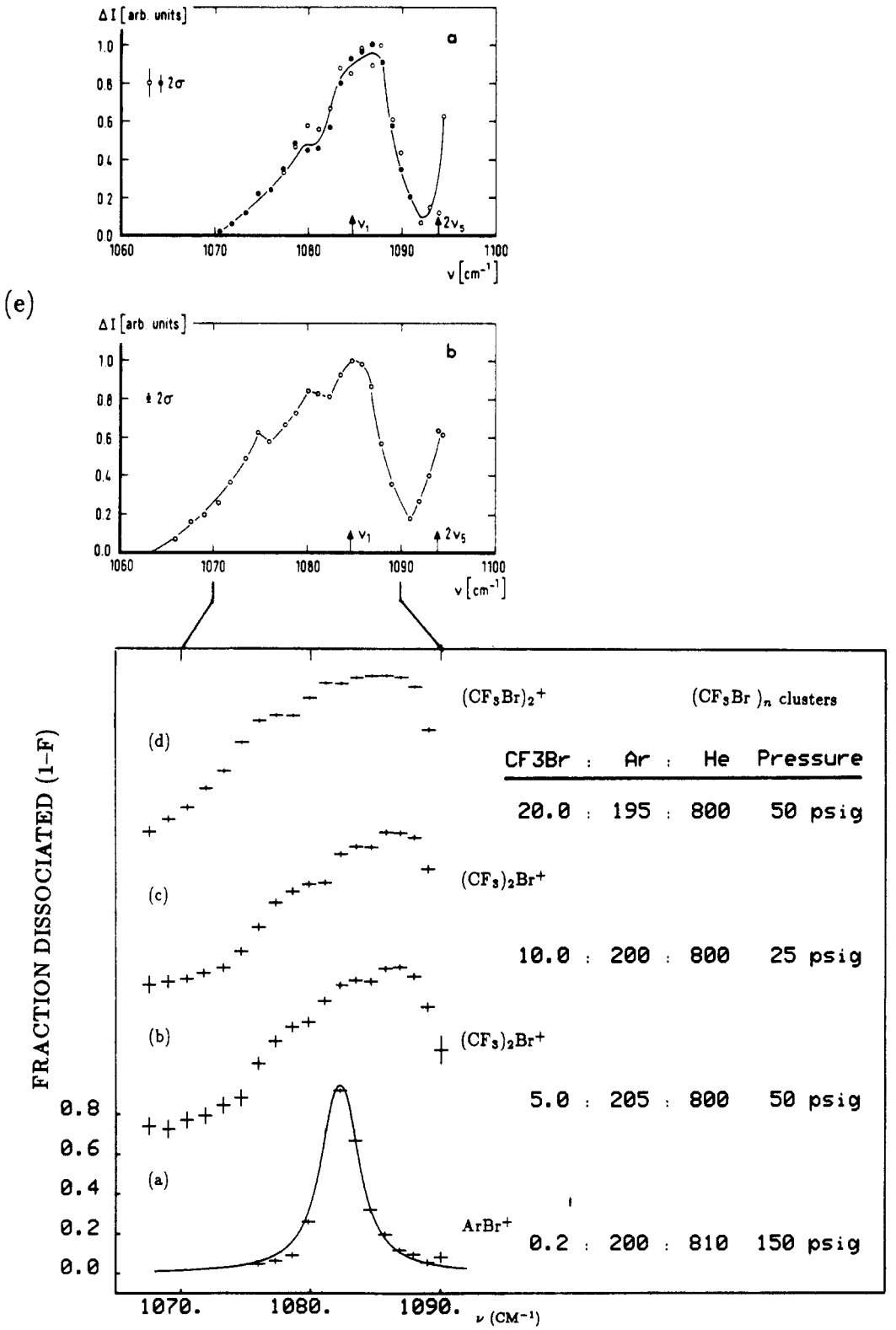

Figure 3. Predissociation profiles of CF_3Br dimers.[62] (a) Ar–CF_3Br profile, ion mass $ArBr^+$. (b,c) The spectra of $(CF_3Br)_2$ obtained at fragment ion mass: (b) $(CF_3)_2Br^+$ (m/e 217); (c) $(CF_3Br)_2^+$. (d,e) The $(CF_3Br)_2$ spectra of Geraedts et al.[60] are included for comparison.

they represent spectra of the dimer, free of contributions from larger complexes.

The spectrum of Ar–CF_3Br, detected by dissociation monitored on the $ArBr^+$ fragment ion, is red-shifted from the CF_3Br gas phase ν_1 absorption by 1.5–2.5 cm^{-1} (Figure 3a). The frequency shift can only be due to electrostatic interaction between the oscillating dipole and the polarizable rare gas atom,[50] as the resonant dipole–dipole transition responsible for splitting the ν_3 absorption in the SF_6 and SiF_4 dimer spectra (vide supra) is not operative in Ar–CF_3Br.

The remainder of Figure 3 displays the dissociation profiles of $(CF_3Br)_2$: parts b and c were determined in our lab, and parts d and e were determined by Geraedts et al.[60] Since the latter spectra were obtained by using mixtures without Ar, we can assign the central feature (1083 cm^{-1}) in parts b and c of Figure 3 as due to $Ar_n(CF_3Br)_2$, $n > 1$, clusters. The two remaining features (1080 and 1086 cm^{-1}) are due to the CF_3Br dimer and are interpreted (vide infra) as indicative of C–F

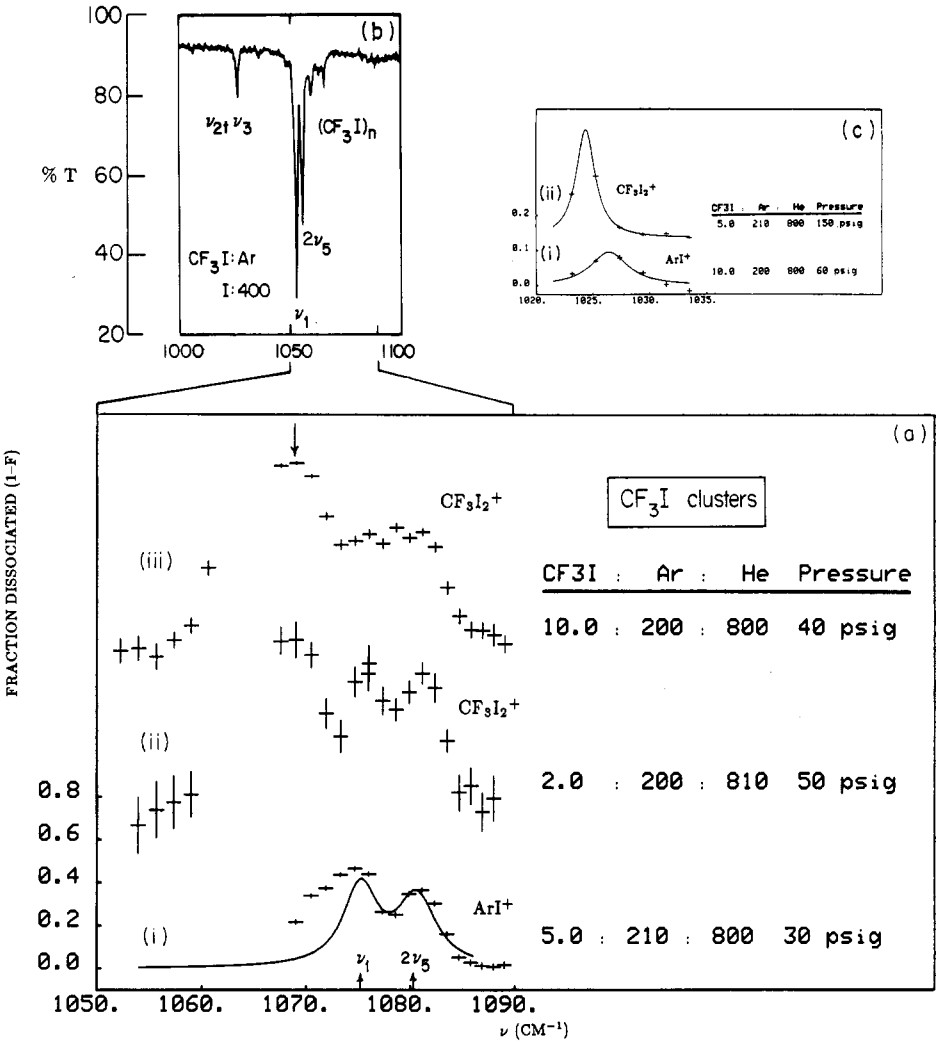

Figure 4. Predissociation profiles of clusters containing CF_3I. (a) In the 1075 cm^{-1} region, both ν_1 and $2\nu_5$ modes, coupled by Fermi resonance, are observed in the cluster dissociation spectra of (i) Ar–CF_3I and (ii,iii) $(CF_3I)_2$ van der Waals dimers. Additional CF_3I dimer features (marked with an arrow) suggest the presence of "free" and "bonded" C–F stretches in $(CF_3I)_2$. (b) Single dissociation peaks are observed for excitation in the $\nu_2 + \nu_3$ combination band region of CF_3I complexes. (c) The IR absorption spectrum of matrix-isolated CF_3I in Ar,[63] showing the $\nu_1/2\nu_5$ pair, $\nu_2 + \nu_3$ combination band, and $(CF_3I)_n$ cluster absorptions (at higher frequency than the monomer).

stretch vibrations from inequivalent CF_3Br molecules: "free" and "bound" moieties analogous to the distinct hydrogen stretches observed for $(HF)_2$.[8] An additional band (not fully resolved) is observed in the spectra of Geraedts et al.,[60] which may be due either to the $2\nu_5$ transition or larger $(CF_3Br)_n$ clusters. If assigned to $2\nu_5$, the intensity appears enhanced compared to that expected from the gas-phase $2\nu_5$:ν_1 intensity ratio.[60]

The ν_1 predissociation spectra of CF_3I clusters are displayed in Figure 4, together with the IR absorption spectrum of CF_3I in an Ar matrix.[63] The Ar–CF_3I dimer spectrum (Figure 4a(i)) exhibits two resolved features (1074.6 and 1080.5 cm^{-1}) whereas the Ar–CF_3Br dimer spectrum showed only a single peak: the two features correspond to the ν_1 and $2\nu_5$ transitions in CF_3I monomer, red-shifted by $\sim$1 cm^{-1}. As deduced from dissociation spectra of Kr–CF_3I dimer in this region (not shown[62]), larger Ar_n–CF_3I clusters (n > 1) also contribute to the displayed spectrum. The $2\nu_5$:ν_1 ratio is unperturbed from that observed in the matrix or in the gas phase.

The dissociation spectrum of CF_3I dimer in this wavelength region suggests structural information on $(CF_3I)_2$ and $(CF_3Br)_2$. In Figure 4a(ii–iii), the $(CF_3I)_2$ spectrum exhibits a nearly unperturbed $\nu_1/2\nu_5$ doublet and a strongly perturbed vibration near 1069 cm^{-1}, corresponding to "free" and "bound" vibrations present in the dimer. Although not completely resolved, this latter feature is shifted at least 7 cm^{-1} to the red of the gas-phase absorption value of CF_3I. Note also that, for both $(CF_3I)_2$ and $(CF_3Br)_2$, the dimer dissociation spectra are found at lower frequency than the gas-phase absorption, while the dimer absorption frequencies in Ar matrices are observed at higher frequency. Dissociation following excitation of the $\nu_2 + \nu_3$ combination mode in CF_3I dimers is also observed (Figure 4c(i and ii)) in this region (1027 cm^{-1}).

Certainly the widths of the CF_3I and CF_3Br dimer profiles can set lower limits on the lifetimes of the excited vibrations (in the picosecond range), but the presence of narrow spectral features indicative of longer lived species may not be apparent in the CO_2 laser photodissociation spectra. That the integrated dissociation intensity is only 30–50% that expected from the absorption intensity of the monomer indicates either that narrow features are in fact present or that the transitions may be fluence broadened. Since the rotational congestion in these heavy molecules will be small

and given the large fraction of dimers which can be dissociated with the narrow band (150 MHz) radiation, the lifetimes are likely within an order of magnitude ($\tau < 10^{-11}$ s) of the established limit. The use of other detection techniques may be necessary to eliminate the possible contributions of larger clusters to the spectra. However, with low-lying vibrational levels in the monomers as well as a higher density of rotational levels, one might expect that the vibrational lifetimes of these dimers would be less than that for $(C_2H_4)_2^*$ but this is certainly not the case as gleaned from the line widths of the reported CF_3I and CF_3Br dimer spectra.

G. H_2O Dimer

A highly structured dissociation spectrum has been reported for the H_2O dimer in the O–H stretch (3200–3800 cm^{-1}) region.[66,67] The spectrum which was obtained using pulsed radiation (~2 cm^{-1} resolution)[66] is quite similar to that recorded using a CW narrow band (150 MHz) laser.[67] High resolution study of the observed bands together with spectral simulation using the known structure[68] would likely provide important dynamical information from the line widths.

H. C_6H_6 Dimer

Two groups have recently reexamined the infrared photodissociation of the benzene dimer. Nishiyama and Hanazaki[69] have excited the in-plane C–H bending mode at 1040 cm^{-1}, ν_{18}, and have measured the product translational energy distribution. They find an average translational energy release of 50 cm^{-1} which they estimate to be one-sixth of the total available product energy. They note that this fraction is very similar to what one would expect from a statistical model for the dissociation mechanism. Johnson, et al.[70] have also measured the translational energy release and obtain a slightly higher average value, 80 cm^{-1}. They assume a deeper attractive well in the dimer which results in an estimate of 33–56% for the fraction of product energy which appears in translation. While the experimental results differ with respect to that predicted from a statistical model for energy release, it is interesting that both estimates for the fraction of product energy in translation are higher than previous results for C_2H_4 dimer[71] and OCS dimer.[42]

VI. Large Clusters

Since our previous review,[1] a good deal of understanding has been gained regarding the infrared spectra of large clusters. Work in this field can be divided into two areas: (a) rare gas clusters which contain an infrared chromophore, such as Ar_n–CH_3F, and (b) homogeneous molecular clusters, such as $(H_2O)_n$, in which $n \gg 2$. The bulk of the present section focuses on the former topic.

Let us first define useful terminology which was not necessary for description of the dimers. Consider the schematic drawing of a 12-atom cluster depicted in Figure 5. With clusters of, e.g., Ar_n, with $n > 12$, both a "matrix" and a "surface" site can be distinguished. In the first cluster (Figure 5a), the impurity or dopant species (hatched) is surrounded by a nearly complete icosahedral shell of atoms. The smallest cluster which might simulate a matrix environment would thus require at least 12 atoms to encompass a small molecule. Cluster-type a thus represents a "matrix" cluster. A "surface" site in this cluster size (Figure 5b) has less than a complete shell of atoms surrounding it. Note also that all clusters below the first complete shell size ($n = 13$) will have only "surface" sites. As the number of atoms and complete solvation shells in the cluster increases, the number of fully solvated matrix sites increases.

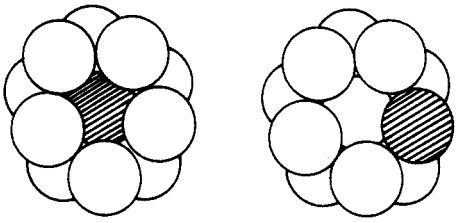

Figure 5. Schematic of a 12-atom cluster, showing (a) "matrix"; (b) "surface" sites.

The infrared spectra of both chromophore-doped rare gas and homogeneous molecular clusters are expected to be sensitive to the site of the absorber, as is the case in matrix-isolation spectroscopy, and this is in fact observed. An additional consideration in the case of molecular clusters is the relative orientation of the monomers: as the size of the crystal grows larger and approaches the bulk limit, the intermolecular structure will tend toward the packing geometry of the crystalline solid.

A. Rare Gas Clusters

Gough et al.[12] have demonstrated the ability to differentiate the infrared spectra of chromophores imbedded within a large rare gas cluster from those at the surface of the cluster. They have introduced a "pick-up" technique, in which the chromophore is attached to a preformed rare gas cluster. While the ν_3 spectra of Ar_n–SF_6 clusters prepared in a conventional supersonic expansion[72] show an absorption analogous to SF_6 in an Ar matrix, the spectrum of Ar clusters with "pick-up" SF_6 molecules exhibits enhanced intensity at a frequency between the gas-phase free SF_6 absorption and that of SF_6 isolated in Ar matrix. The SF_6 chromophore resides preferentially on the surface of the Ar cluster when prepared in this novel way.[12]

Polar chromophores (e.g., CH_3F) deposited on the surface of a rare gas cluster may cause reorganization of the cluster due to the driving force of the solvation energy (vide infra). While this mobility may make it difficult to isolate clusters with surface-site chromophores, it might also provide a simple way to distinguish the phase of the cluster. For instance, CH_3F introduced directly at the surface of a warm "liquid" Ar cluster might efficiently reorient and yield the infrared spectra of the matrix site closer, whereas a cold "solid" Ar crystal may hinder the diffusion of CH_3F into the bulk so the CH_3F chromophore would exhibit a "surface" site spectrum.[13b]

Scoles et al.[72] have reported the observation of narrow features in the dissociation profile of large Ar clusters containing CH_3F. We have found[1,13] that an especially intense feature is exhibited by "matrix-type" clusters

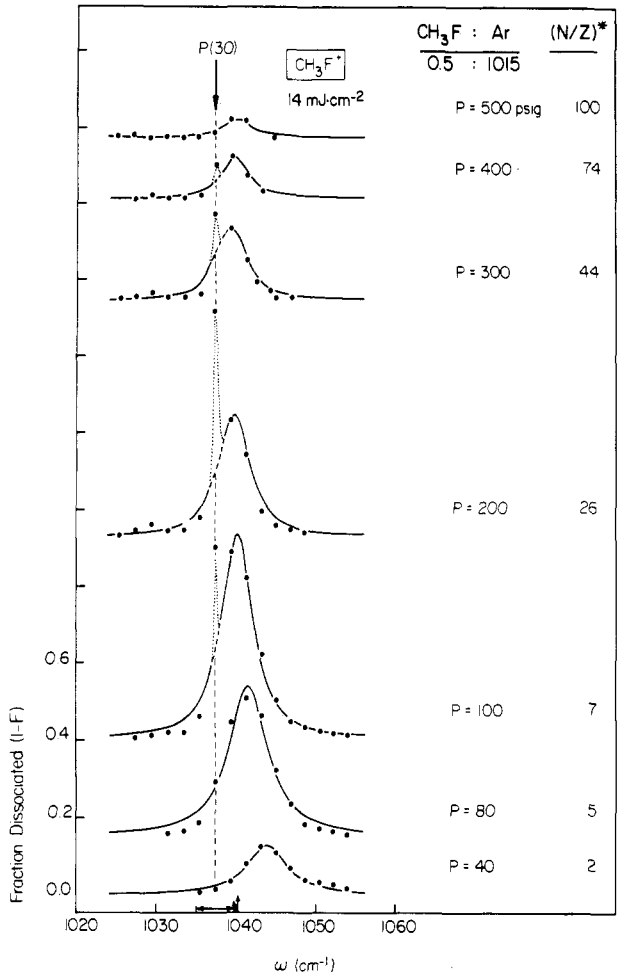

Figure 6. Pressure dependence of Ar_n–CH_3F clusters as detected at m/e 34 (CH_3F^+).[13] Between 100 and 300 psig, the fraction of clusters dissociated at 1037.4 cm^{-1} increases dramatically, attributed to the appearance of clusters with "matrix"-site CH_3F absorptions. The "surface"-site CH_3F absorption at higher frequency persists in spectra of larger clusters (p = 400–500 psig) while the matrix feature disappears.

of a specific size. This dissociation feature was red-shifted from the gas phase ν_3 frequency, and further red-shifted (~2.5 cm^{-1}) *beyond* the ν_3 absorption of CH_3F isolated in a rare gas matrix. We have sought to extend our understanding of the Ar/CH_3F system, both by studying other cluster systems with CH_3F as the chromophore and by using C_2H_4 as the infrared absorbing guest in rare gas and molecular clusters.[13] There is also much experimental and theoretical characterization of the distribution, structure, and dynamics of large rare gas clusters which serves as a solid foundation for interpretation of the infrared data. Here we summarize our findings using spectra from the Ar/CH_3F and Ar/C_2H_4 cluster systems as examples.[13b]

Employing the spectrometer described in previous studies,[50] we produce large Ar clusters with a single CH_3F or C_2H_4 chromophore and monitor the CO_2 laser-induced depletion of clusters as detected with an electron impact ionization quadrupole mass spectrometer. The spectra are thus mainly sensitive to absorption of radiation which produces dissociation (or evaporation) of the cluster. Figure 6 shows the dissociation spectra obtained at mass 34 (CH_3F^+) as a function of source pressure of an Ar/CH_3F mixture. Note that because of the fragmentation induced by ionization of the clusters,[73] laser-induced depletion of clusters can be observed at the (nominal) monomer ion mass, CH_3F^+. Moreover, the resultant infrared spectrum acts as a probe of the entire cluster distribution, much the same way as with bolometric detection.[12,72]

We observe that three regimes of cluster size can be distinguished using the IR dissociation spectra. Using the listed $(N/Z)^*$ values, computed[13a] from the clustering studies of Hagena,[74] as rough guides to the mean of the neutral cluster distribution, a "small" cluster regime (figure 6, P = 40 and 80 psig) can be associated with clusters which have less than one complete Ar shell. In this regime, the frequency shift of the CH_3F ν_3 vibration per additional Ar atom is less than the line width, so the center of the dissociation profile appears to shift continuously to lower frequency as the source pressure (and the mean of the cluster distribution) increases. The "moderate" cluster size regime is associated with clusters filling a second Ar shell, Ar_n–CH_3F, $12 < n < 54$. A narrow and intense "matrix" dissociation feature is observed for clusters which have the CH_3F chromophore solvated within the cluster. The "surface" site absorption feature, which is characteristic of clusters having an incomplete solvation shell, is dominant at low source pressure and becomes less dominant as the number of atoms in the cluster increases. In the "large" cluster regime, (Figure 6, P = 300–500 psig), the dissociation intensity of both the matrix and surface features are quenched, most dramatically with the former. Only the broad surface site absorption is observed in dissociation at the highest backing pressures. To summarize, we observe three clustering regions characterized by, respectively: (1) red-shifting of a single surface-site CH_3F dissociation band, (2) appearance of a narrow and intense matrix-site CH_3F feature, and (3) disappearance of the matrix feature and quenching of the dissociation signal of the surface-site chromophore.

The matrix-site feature, coincident only with a single CO_2 laser line (1037.43 cm^{-1}) is indicative of a specific range of neutral clusters, as is shown by the spectra in Figure 7. While ionization causes many large cluster sizes to fragment to an ion mass, the mass filtering capability of the mass spectrometer can be utilized to eliminate the contribution of clusters smaller than the monitored ion mass to the dissociation profile. The spectra taken at ion mass Ar_5–CH_3F^+ (Figure 7a) demonstrate that neutral clusters smaller than Ar_5–CH_3F do not give rise to the matrix-site absorption peak. For dissociation monitored on the Ar_9–CH_3F^+ ion mass (Figure 7b, P = 200 psig), the intensity ratio between the "matrix" and "surface" site absorptions is greater that that for CH_3F^+ ion mass detection (Figure 6, P = 200 psig). In the former case, contributions from Ar_n–CH_3F ($n < 8$) clusters have been filtered out of the infared spectrum. That the narrow peak at 1037.6 cm^{-1} has a larger frequency shift than the "surface" feature corroborates our assignment of the matrix-site feature as being due to Ar clusters with a solvated CH_3F chromophore. Finally, the matrix-site feature is characteristic of a narrow range of Ar_n–CH_3F clusters, since there is a great difference in the IR dissociation spectra taken under the same expansion conditions at Ar_9–CH_3F^+ and Ar_{12}–CH_3F^+ (Figure 7b,c).

The fate of the matrix-site feature at high source pressure cannot be unequivocally determined due, in

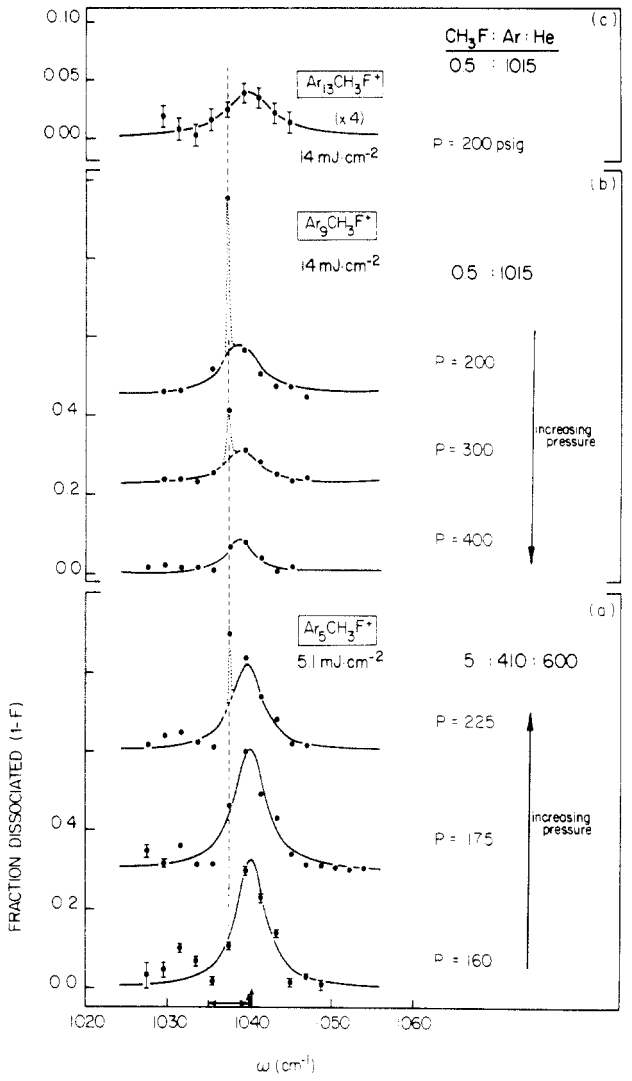

Figure 7. Predissociation spectra of the Ar/CH_3F cluster system obtained from various fragment ion masses.[13] The set of spectra indicate (i) the "matrix" feature is associated with a range of cluster sizes; (ii) specificity is exhibited in the ionization of the large neutral clusters.

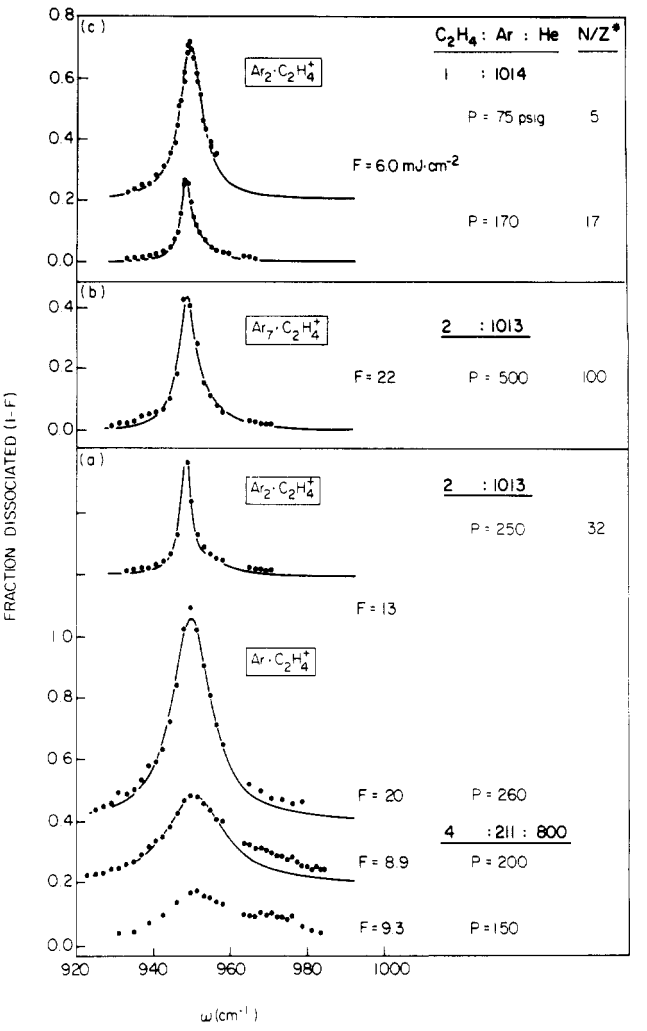

Figure 8. Dissociation profiles of Ar clusters using C_2H_4 as the IR absorbing chromophore.[13] No sharp "matrix" features, analogous to those seen in the Ar/CH_3F cluster system, are observed, under similar expansion conditions.

part, to the coarse grid of CO_2 laser lines in this region ($\sim$2 cm^{-1}). The CH_3F ν_3 absorption maximum must eventually shift to 1040 cm^{-1}, the matrix, isolation value, as the Ar microcrystallite attains properties of the bulk. Quenching of the dissociation is also likely, however, as the cluster size increases. The spectra of large Kr and N_2 clusters containing a CH_3F chromophore[13a] give evidence for the expected frequency shift, and so it is reasonable to surmise that large matrix-site Ar_nCH_3F clusters have absorptions that fall between the available laser lines. Tunable lasers available in other regions of the infrared spectrum would lend further insight into this question. Also, bolometric detection of the clusters would discern whether the chromophore still absorbs radiation even though the cluster dissociation may be quenched.

We undertook the study of large clusters containing C_2H_4 as the chromophore in an attempt to track the frequency shift of the matrix-site feature, the spacing between CO_2 and N_2O laser lines is narrower ($\sim$0.75 cm^{-1}) in the C_2H_4 ν_7 region. Surprisingly, with three cluster systems (Ar, N_2, and CH_4), no evidence for narrow spectral features is observed.[13a] Dissociation spectra of Ar_n–C_2H_4 clusters are shown in Figure 8.

Although there is some narrowing of the dissociation profile as the size of the clusters increases, no sharp features can be distinguished. Two effects could be responsible for this observation. The lifetime of the excited C_2H_4 ν_7 vibration in the "matrix" Ar clusters may be much longer than the CH_3F ν_3 vibration and thus the resultant narrow transitions would likely not be observed in the dissociation spectra. We feel a more plausible explanation is that the polar CH_3F molecule is preferentially situated in the matrix site of the cluster, in which maximum solvation energy can be attained, whereas this driving force is not as dominant for the nonpolar C_2H_4 chromophore. If the C_2H_4 dopant is statistically distributed among the cluster sites, there will not be a significant fraction of Ar clusters containing C_2H_4 in a matrix site for the cluster sizes prepared under these beam conditions. Indeed, the relatively small neutral cluster size at which the "matrix" absorption peak is observed in the spectra of Ar_nCH_3F clusters indicates that there is a significant preference for CH_3F to be fully solvated within the clusters.

While IR chromophores can be used to probe weakly bound rare gas clusters through laser-induced evaporation, the exact nature of the matrix- and surface-site transition line widths can be further clarified. Information about the rare gas cluster environment can be obtained, but the chromophore itself can affect the

orientation of the cluster. The application of continuously tunable lasers or time-resolved techniques to these systems should prove quite fruitful toward resolving some of the questions which have been raised by the studies in this field.

B. Homogeneous Molecular Clusters

One can utilize the synthetic capabilities of the supersonic expansion to grow successively larger clusters from the monomer and the clusters should exhibit condensed phase properties, such as in their infrared absorption spectra. Significant progress in interpretation of the observed bandshapes as a function of cluster size has been shown by Watts, Miller, and co-workers[39,67,75] for $(H_2O)_n$ and $(N_2O)_n$ clusters. Observed bands in the $\nu_1 + \nu_3$ region spectrum of $(N_2O)_n$ clusters were successfully modeled and suggest that even moderate-size clusters (e.g., $(N_2O)_{55}$) will exhibit a wide range of absorption bands corresponding to multiple isomeric structures for the clusters.[38b] Using various simulations, features in the O–H stretch spectra of small $(H_2O)_n$ clusters could be associated with stable structures.[75]

C. Isotope Separation with Clusters

An extensive photochemical study[14,76-78] of the IR absorption of Ar clusters containing SF_6 has been conducted, with special attention directed toward separation of $^{32}SF_6$ and $^{34}SF_6$ isotopomers. Even though a variety of mixed $Ar_n(SF_6)_m$ clusters with overlapping absorption spectra[76] are present under most beam conditions, significant spatial separation of the isotopomers can be achieved. The vibrational predissociation[14] of mixed $Ar_n(SF_6)_m$ clusters (analogous to the dimer dissociation studies reviewed above) and the selective inhibition of condensation[77] of SF_6 into Ar clusters have proven effective, both separately and in tandem.[78]

VII. Summary

This review helps to illustrate how studies of the infrared spectra of molecular dimers and larger clusters provide fascinating examples of intramolecular energy redistribution. Perhaps the most surprising advance in the past several years is the discovery that even for polyatomic systems with many degrees of freedom there can be long-lived vibrationally metastable states. We thus have hope that through detailed spectroscopic and dynamic (e.g., pump–probe) studies, the mechanism for intramolecular vibrational relaxation on a single electronic surface can be understood in great detail. Although this problem is far from being solved for all but the most simple molecules, it is gratifying to see evidence that a solution is indeed attainable. When detailed mechanisms of relaxation and dissociation for a select set of van der Waals molecules are understood, this insight may perhaps be extended to larger systems for which detailed spectra cannot be obtained.

This review article, as well as the others in this volume, suggest that there will be many practical applications of molecular and ionic clusters. The importance of isotope separation schemes in obvious. Ultimately, the understanding of the effects of cluster size in the modeling of chemical reactions of adsorbed molecules on surfaces may prove to be even more important.

Acknowledgments. We would like to acknowledge the U.S. Department of Energy for financial support throughout our investigations. K.C.J. would also like to thank the Laboratoire de Photophysique Molécular, Université de Paris-Sud, for hospitality during the preparation of this manuscript, and would like to acknowledge a Fulbright Fellowship for financial support.

References

(1) Janda, K. C. *Adv. Chem. Phys.* **1985**, *60*, 201.
(2) Levy, D. H. *Adv. Chem. Phys.* **1981**, *47*, 323.
(3) Beswick, J. A.; Jortner, J. *Adv. Chem. Phys.* **1981**, *47*, 363.
(4) Ewing, G. E. *Faraday Discuss. Chem. Soc.* **1982**, *73*, 325.
(5) Brinza, D. E.; Swartz, B. A.; Western, C. M.; Janda, K. C. *J. Chem. Phys.* **1983**, *79*, 1541.
(6) LeRoy, R. J. In *Resonances in Electron-Molecule Scattering, van der Waals Molecules and Reactive Chemical Dynamics*; Truhlar, D. G., Ed.; American Chemical Society: Washington, D.C., 1984; p 231.
(7) Howard, B. J.; Pine, A. S. *Chem. Phys. Lett.* **1985**, *122*, 1.
(8) (a) Pine, A. S.; Lafferty, W. J. *J. Chem. Phys.* **1983**, *78*, 2154. (b) Pine, A. S.; Lafferty, W. J.; Howard, B. J. *J. Chem. Phys.* **1984**, *81*, 2939.
(9) Ohashi, N.; Pine, A. S. *J. Chem. Phys.* **1984**, *81*, 73.
(10) Hayman, G. D.; Hodge, J.; Howard, B. J.; Muenter, J. S.; Dyke, T. R. *Chem. Phys. Lett.* **1985**, *118*, 12.
(11) Fraser, G. T.; Nelson, D. D., Jr.; Charo, A.; Klemperer, W. *J. Chem. Phys* **1985**, *82*, 2535.
(12) Gough, T. E.; Mengel, M.; Rowntree, P. A.; Scoles, G. *J. Chem. Phys.* **1985**, *83*, 4958.
(13) (a) Celii, F. G.; Janda, K. C. submitted for publication in *J. Phys. Chem.* (b) Celii, F. G.; Janda, K. C., submitted for publication in *Chem. Phys. Lett.*
(14) Philippoz, J.-M.; Zellweger, J.-M.; van den Bergh, H.; Monot, R. *J. Chem. Phys.* **1984**, *88*, 3936.
(15) LeRoy, R. J.; Corey, G. C.; Hutson, J. M., *Faraday Discuss. Chem. Soc.* **1982**, *73*, 339.
(16) McKellar, A. R. W. *Faraday Discuss. Chem. Soc.* **1982**, *73*, 89.
(17) Buck, U. *Faraday Discuss. Chem. Soc.* **1982**, *73*, 187.
(18) Kidd, I. F.; Balint-Kurti, G. G. *J. Chem. Phys.* **1985**, *82*, 93.
(19) (a) Marshall, M. D.; Charo, A.; Leung, H. O.; Klemperer, W. *J. Chem. Phys.* **1985**, *83*, 4924. (b) Ray, D.; Robinson, R.. L.; Gwo, D.; and Saykally, R. J. *J. Chem. Phys.* **1986**, *84*, 1171.
(20) Hutson, J. M. *J. Chem. Phys.* **1984**, *81*, 2357.
(21) (a) Dyke, T. R.; Howard, B. J.; Klemperer, W., *J. Chem. Phys.* **1972**, *56*, 2442. (b) Howard, B. J.; Dyke, T. R.; Klemperer, W. *J. Chem. Phys.* **1984**, *81*, 5417.
(22) Gutowsky, H. S.; Chuang, C.; Keen, J. D.; Klots, T. D.; Emilsson, T. *J. Chem. Phys.* **1985**, *83*, 2070.
(23) Pine, A. S.; Howard, B. J. *J. Chem. Phys.* **1986**, *84*, 590.
(24) Micheal, D. W.; Dykstra, C. E.; Lisy, J. M. *J. Chem. Phys.* **1984**, *81*, 5998.
(25) Barton, A.; Howard, B. J. *Faraday Discuss. Chem. Soc.* **1982**, *73*, 45.
(26) DeLeon, R. L.; Muenter, J. S. *J. Chem. Phys.* **1984**, *80*, 6092.
(27) Vernon, M. F.; Lisy, J. M.; Kwok, H.-S., Krajinovich, D. J.; Tramer, A.; Shen, Y.-R.; Lee, Y. T. *J. Chem. Phys.* **1981**, *75*, 4733.
(28) (a) Andrews, L. *J. Phys. Chem.* **1984**, *88*, 2940. (b) Andrews, L. *J. Chem. Phys.* **1984**, *81*, 3451.
(29) (a) Ewing, G. E. *J. Chem. Phys.* **1980**, *72*, 2096. (b) Halberstadt, N.; Brechignac, Ph.; Beswick, J. A.; Shapiro, M. *J. Chem. Phys.* **1986**, *84*, 170.
(30) Gentry, W. R. In *Resonances in Electron-Molecule Scattering, van der Waals Molecules and Reactive Chemical Dynamics*; Truhlar, D. G.; Ed.; American Chemical Society: Washington, D.C. 1984; p 289.
(31) Kyrö, E.; Warren, R.; McMillan, K.; Eliades, M.; Danzeisin, D.; Shoja-Chaghervand, P.; Lieb, S. G.; Bevan, J. W. *J. Chem. Phys.* **1983**, *78*, 5881.
(32) (a) Hopkins, G. A.; Maroncelli, M.; Nibler, J. W.; Dyke, T R. *Chem. Phys. Lett.* **1985**, *114*, 97. (b) Maroncelli, M.; Hopkins, G. A.; Nibler, J. W.; Dyke, T. R. *J. Chem. Phys.* **1985**, *83*, 2129.
(33) König, F.; Osterlin, P.; Byer, R. L. *Chem. Phys. Lett.* **1982**, *88*, 477.
(34) (a) Dinnerman, C. E.; Ewing, G. E. *J. Chem. Phys.* **1970**, *53*, 626. (b) Dinnerman, C. E.; Ewing, G. E. *J. Chem. Phys.* **1971**, *54*, 3660.
(35) Menoux, V.; LeDoucen, R.; Haeusler, C.; Deroche, J. C. *Can. J. Phys.* **1984**, *62*, 322.
(36) Brechignac, Ph.; DeBenedictis, S.; Halberstadt, N.; Whitaker, B. J.; Avrillier, S. *J. Chem. Phys.* **1985**, *83*, 2064.
(37) Western, C. M.; Langridge-Smith, P. R. R.; Howard, B. J.; Novick, S. E. *Mol. Phys.* **1981**, *44*, 145.

(38) (a) Gough, T. E.; Miller, R. E.; Scoles, G. *J. Chem. Phys.* **1978**, *69*, 1588. (b) Miller, R. E.; Watts, R. O. *Chem. Phys. Lett.* **1984**, *105*, 409.
(39) Miller, R. E.; Watts, R. O.; Ding, A. *Chem. Phys.* **1984**, *83*, 155.
(40) Miller, R. E.; Vorhalik, P. F.; Watts, R. O. *J. Chem. Phys.* **1984**, *80*, 5453.
(41) Fischer, G.; Miller, R. E.; Vorhalik, P. F.; Watts, R O. *J. Chem. Phys.* **1985**, *83*, 1471.
(42) Hoffbauer, M. A.; Liu, K.; Giese, C. F.; Gentry, W. R. *J. Phys. Chem.* **1983**, *87*, 2096.
(43) (a) Buck, U.; Meyer, F. *Phys. Rev. Lett.* **1984**, *52*, 109. (b) Huisken, F.; Meyer, H.; Laurenstein, C.; Sroka, R.; Buck, U. *J. Chem. Phys.* **1986**, *84*, 1042.
(44) Western, C. M.; Casassa, M. P.; Janda, K. C. *J. Chem. Phys.* **1984**, *80*, 4781.
(45) Liu, W. L.; Kolenbrander, K.; Lisy, J. M. *Chem. Phys. Lett.* **1984**, *112*, 585.
(46) Haynam, C. A.; Brumbaugh, D. V.; Levy, D. H. *J. Chem. Phys.* **1984**, *81*, 2282.
(47) Hoffbauer, M. A.; Liu, K.; Giese, C. F.; Gentry, W. R. *J. Chem. Phys.* **1983**, *79*, 192.
(48) Gibson, L. L.; Schatz, G. C. *J. Chem. Phys.* **1985**, *83*, 3433.
(49) Geraedts, J.; Stolte, S.; Reuss, J. *Z. Phys. A* **1982**, *304*, 167.
(50) Casassa, M. P.; Western, C. M.; Celii, F. G.; Brinza, D. E.; Janda, K. C. *J. Chem. Phys.* **1983**, *79*, 3227.
(51) Hutson, J. M.; Clary, D. C.; Beswick, J. A. *J. Chem. Phys.* **1984**, *81*, 4474.
(52) Howard, M. J.; Burdenski, C. F.; Giese, C. F.; Gentry, W. R. *J. Chem. Phys.* **1984**, *80*, 4137.
(53) Pople, J. A. *Faraday Discuss. Chem. Soc.* **1982**, *73*, 7.
(54) Gentry, W. R., In Electron At. Collisions, Proc. Int. Conf., 11th, 1979.
(55) Gasassa, M. P.; Bomse, D. S.; Beauchamp, J. L.; Janda, K. C. *J. Chem. Phys.* **1981**, *74*, 5044.
(56) Casassa, M. P.; Western, C. M.; Janda, K. C. "Resonances in Electron-Molecule Scattering, van der Waals Molecules and Reactive Chemical Dynamics; Truhlar, D. G., Ed.; American Chemical Society: Washington, D.C., 1984 p 305.
(57) Mitchell, A.; McAuliffe, M. J.; Giese, C. F.; Gentry, W. R. *J. Chem. Phys.* **1985**, *83*, 5343.
(58) King, D. S. Stephenson, J. C. *J. Chem. Phys.* **1985**, *82*, 5286.
(59) Hoffbauer, M. A.; Giese, C. F.; Gentry, W. R. *J. Phys. Chem.* **1984**, *88*, 181.
(60) Geraedts, J.; Snels, M. N. N.; Stolte, S.; Reuss, J. *Chem. Phys. Lett.* **1984**, *106*, 377.
(61) (a) Geraedts, J.; Setiadi, S.; Stolte, S.; Reuss, J. *J. Chem. Phys.* **1981**, *78*, 277. (b) Geraedts, J.; Waayer, M.; Stolte, S.; Reuss, J. *Faraday Discuss. Chem. Soc.* **1982**, *73*, 375.
(62) Celii, F. G. Ph.D. Thesis, California Institute of Technology, 1985.
(63) Jacox, M. E., private communication.
(64) Fuss, W. *Spectrochim. Acta* **1982**, *38A*, 829.
(65) Bürger, H.; Burczyk, L.; Bielefeldt, D.; Willner, H.; Ruoff, A.; Molt, K., *Spectrochim. Acta* **1979**, *35A*, 875.
(66) Page, R. H.; Frey, J. G.; Shen, Y.-R.; Lee, Y. T. *Chem. Phys. Lett.* **1984**, *106*, 373.
(67) Coker, D. F.; Miller, R. E.; Watts, R. O. *J. Chem. Phys.* **1985**, *82*, 3554.
(68) Dyke, T. R.; Mack, K. M.; Muenter, J. S. *J. Chem. Phys.* **1977**, *66*, 498.
(69) Nishiyama, E.; Hanazaki, I. *Chem. Phys. Lett.* **1985**, *117*, 99.
(70) Johnson, R. D.; Bardenski, S.; Hoffbauer, M. A.; Giese, C. F.; Gentry, W. R. *J. Chem. Phys.* **1986**, *84*, 4624.
(71) (a) Hoffbauer, M. A.; Liu, K.; Giese, C. F.; Gentry, W. R. *J. Chem. Phys.* **1983**, *78*, 5567. (b) Bomse, D. S.; Cross, J. B.; Valentini, J. J. *J. Chem. Phys.* **1983**, *78*, 7175.
(72) Gough, T. E.; Knight, D. G.; Scoles, G. *Chem. Phys. Lett.* **1983**, *97*, 155.
(73) (a) Soler, J. M.; Garcia, N. *Phys. Rev. A* **1983**, *27*, 3300. (b) Soler, J. M.; Garcia, N. *Phys. Rev. A* **1983**, *27*, 3307.
(74) Hagena, O. F. *Surf. Sci.* **1981**, *101*, 106, and references therein.
(75) Reimers, J. R.; Watts, R. O. *Chem. Phys.* **1984**, *85*, 83.
(76) Philippoz, J.-M.; Zellweger, J.-M.; van den Bergh, H.; Monot, R. *Surf. Sci.* **1985**, *156*, 701.
(77) Zellweger, J.-M.; Philippoz, J.-M.; Melinon, P.; Monot, R.; van den Bergh, H. *Phys. Rev. Lett.* **1984**, *52*, 522.
(78) (a) Philippoz, J.-M.; Calpini, B.; van den Bergh, H.; Monot, R. *Helv. Phys. Acta*, in press. (b) Philippoz, J.-M.; Calpini, B.; Monot, R.; van den Bergh, H. *Ber. Bunsen-Ges. Phys. Chem.* **1985**, *89*, 291.